East European Journal of Physics. 2. 398-404 (2025)
DOI:10.26565/2312-4334-2025-2-48 ISSN 2312-4334

COMPUTATIONAL STUDY OF DRUG DELIVERY SYSTEMS WITH RADIONUCLIDE AND FLUORESCENCE IMAGING MODALITIES. III. DOXORUBICIN DELIVERY SYSTEMS BASED ON ALBUMIN AND LYSOZYME

V. Trusova[a]*, U. Malovytsia[a], P. Kuznietsov[b], I. Yakymenko[b], I. Karnaukhov[c], A. Zelinsky[c], B. Borts[c], I. Ushakov[c], L. Sidenko[c], G. Gorbenko[a]

[a]*Department of Medical Physics and Biomedical Nanotechnologies, V.N. Karazin Kharkiv National University 4 Svobody Sq., Kharkiv, 61022, Ukraine*

[b]*O.I. Akhiezer Department for Nuclear Physics and High Energy Physics, V.N. Karazin Kharkiv National University 4 Svobody Sq., Kharkiv, 61022, Ukraine*

[c]*National Science Center "Kharkiv Institute of Physics and Technology", 1, Akademichna Str., Kharkiv, Ukraine*

**Corresponding Author e-mail: valerija.trusova@karazin.ua*

Received March 1, 2025, revised April 24, 2025; accepted May 17, 2025

This study investigates the development of advanced protein-based drug delivery systems for doxorubicin (DOX) by integrating lysozyme into albumin-based carriers, incorporating both radionuclide (technetium-99m complexes) and fluorescence (near-infrared dyes) imaging modalities. Utilizing molecular docking simulations, we examined the binding affinities and sites of technetium-99m complexes and near-infrared fluorescent dyes within these hybrid protein systems. The results demonstrate that the incorporation of lysozyme significantly modulates the binding landscape, enhancing the specificity and stability of technetium complexes and fluorescent dyes. Notably, the binding affinities of indocyanine green were markedly higher in lysozyme-containing systems, suggesting improved imaging capabilities. Additionally, our analysis revealed distinct binding sites for doxorubicin in the presence of different technetium complexes, which could influence drug release and therapeutic efficacy. These findings support the potential of albumin-lysozyme hybrid systems as nanocarriers with dual imaging capabilities for DOX delivery, offering a promising approach to enhance therapeutic efficacy while reducing systemic toxicity in anticancer treatment and contributing to the design of more sophisticated and targeted delivery platforms for cancer therapy.

Keywords: *Protein-based drug delivery nanosystems; Human serum albumin; Lysozyme; Doxorubicin; Technetium complexes; Near infrared dyes; Molecular docking*

PACS: 87.14.C++c, 87.16.Dg

The development of multifunctional effective drug delivery systems remains a critical challenge in modern oncology, where the need for improved therapeutic efficacy must be balanced against the risk of systemic toxicity, particularly for potent but toxic agents like doxorubicin (DOX). Protein-based carriers have emerged as promising platforms due to their intrinsic biocompatibility, structural versatility, and capacity for targeted drug transport [1,2]. These characteristics enable precise control over drug pharmacokinetics and biodistribution while allowing for the incorporation of imaging agents that facilitate real-time monitoring of drug delivery. Among the various proteins explored for this purpose, human serum albumin (HSA) has been extensively studied for its ability to enhance drug solubility, prolong circulation time, and promote tumor accumulation through passive targeting mechanisms [3]. Our previous works established transferrin-albumin hybrids as effective DOX delivery vehicles with integrated imaging capabilities [4,5]. However, lysosomal entrapment and extracellular matrix viscosity may limit the translational potential of such systems in hypoxic solid tumors [6,7]. In response to these potential clinical challenges, we are compelled to explore alternative protein combinations that can overcome these barriers, and in the present contribution we introduce lysozyme (Lz), cationic, membrane-permeabilizing protein with inherent glycosidase activity [8,9], as a strategic partner to HSA in designing the next-generation theranostic platforms. Unlike transferrin receptor-mediated targeting, lysozyme confers unique advantages through pH-dependent structural reconfiguration and enzymatic degradation of bacterial cell wall analogs, a property exploitable in tumor microenvironments enriched with peptidoglycan-mimetic glycoproteins. Using computational modeling approaches, this study aims to characterize the molecular interactions between DOX, albumin, and lysozyme to assess the structural and energetic factors influencing drug loading and stability. Additionally, we explore the potential of these hybrid protein carriers for applications in multimodal imaging, where the incorporation of radiopharmaceutical and fluorescent labels could provide new opportunities for non-invasive tracking of drug biodistribution.

METHODS

Dimeric conformation of human serum albumin (HSA) (PDB ID: 1AO6) was selected as the principal constituent of the constructed protein-based drug delivery systems (PDDS). For PDDS formulation, twelve radiopharmaceuticals

Cite as: V. Trusova, U. Malovytsia, P. Kuznietsov, I. Yakymenko, I. Karnaukhov, A. Zelinsky, B. Borts, I. Ushakov, L. Sidenko, G. Gorbenko, East Eur. J. Phys. 2, 398 (2025), https://doi.org/10.26565/2312-4334-2025-2-48

based on technetium-99m (TCC) were selected [4,5]: [^{99m}Tc]Tc-Sestamibi (TcSES), [^{99m}Tc]Tc-Tetrofosmin (TcTET), [^{99m}Tc]Tc-Medronate (TcMED), [^{99m}Tc]Tc-dimercaptosuccinic acid (TcDMSA), [^{99m}Tc]Tc-diethylenetriaminepentaacetate (TcDTPA), [^{99m}Tc]Tc-mercaptoacetyltriglycine (TcMAG), Pertechnetate [^{99m}Tc]TcO_4^- (TcPER), [^{99m}Tc]Tc-Exametazime (TcEXA), [^{99m}Tc]Tc-diisopropyl iminodiacetic acid (TcDIS), [^{99m}Tc]Tc-ethylene cysteine dimer (TcECD), [^{99m}Tc]Tc-hydrazinonicotinic acid-H6F (TcHYN), and [^{99m}Tc]Tc-Mebrofenin (TcMEB). To enable multimodal imaging with both radionuclide and optical tracking capabilities, these [^{99m}Tc] complexes were combined with four near-infrared (NIR) fluorescent dyes: Methylene Blue (MB), Indocyanine Green (IG), cyanine AK7-5, and squaraine SQ1. Molecular docking analyses were conducted using the HDOCK server to determine the optimal binding sites for technetium-labeled agents, DOX, and fluorescent dyes in HSA-Lz protein assemblies. Prior to docking, molecular dynamics (MD) simulations of 1 ns were performed to refine the structures of HSA dimers and their complexes with lysozyme (Lz). Ligand structures were created in MarvinSketch (version 18.10.0) and underwent geometry optimization using Avogadro (version 1.1.0). The best docking conformations were visualized with UCSF Chimera (version 1.14) and analyzed via the Protein-Ligand Interaction Profiler [10].

RESULTS AND DISCUSSION

Our previous studies have explored the potential of albumin-based drug delivery systems for doxorubicin (DOX) with integrated radionuclide and fluorescence imaging modalities [4,5]. Specifically, our first work demonstrated that human serum albumin (HSA) can serve as an effective carrier for DOX, forming stable complexes with technetium-99m-based radiopharmaceuticals and near-infrared fluorescent (NIR) dyes. Molecular docking and molecular dynamics simulations revealed that these multimodal nanocarriers exhibit strong binding affinities and structural stability, supporting their potential use in theranostic applications. Expanding on this approach, our second paper from this series introduced transferrin (TRF) as an additional protein component, investigating its role in enhancing the targeting capabilities of albumin-based drug delivery platforms. The findings indicated that HSA-TRF complexes maintain favorable interactions with TCC and fluorescent dyes, highlighting their promise for improving the therapeutic efficacy and specificity of DOX delivery. The present study focuses on drug delivery systems based on albumin and lysozyme, aiming to further refine the design of protein-based carriers by evaluating their binding interactions and stability in multimodal imaging.

As illustrated in Fig. 1, left panel, the best docking scores (BDS) for TCC binding to the albumin-lysozyme (HAS-Lz) complexes reveal a hierarchy of affinities: HSA + Lz - TcHYN > TcDIS > TcMEB > TcDTPA ~ TcTET ~ TcDMSA ~ TcSES ~ TcMED ~ TcECD ~ TcMAG ~ TcEXA > TcPER.

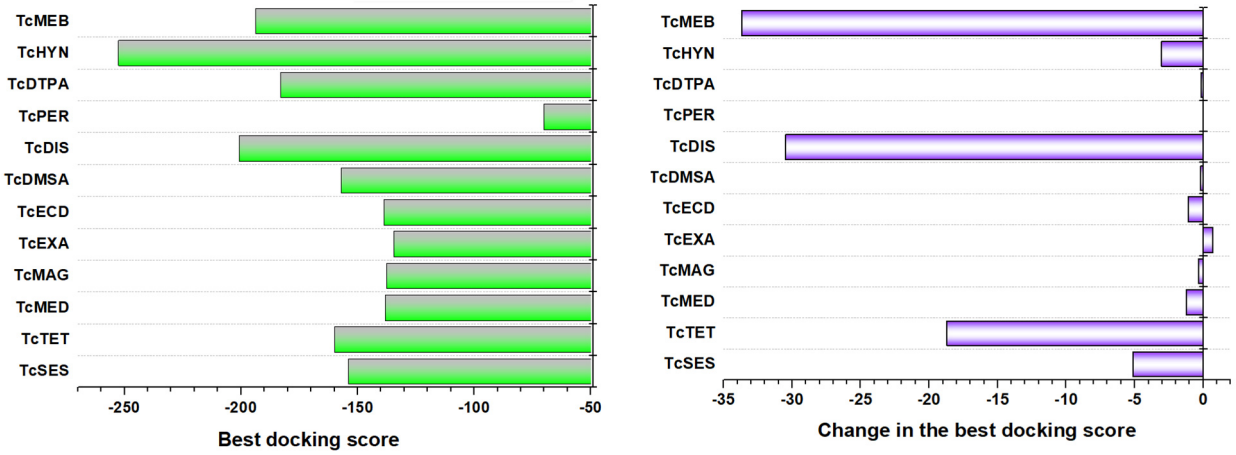

Figure 1. Absolute values (left panel) and changes (right panel) in the best docking score values obtained for the TCC complexes with HSA in the absence and presence of Lz

Interestingly, the BDS value for the HSA-Lz complex was estimated to be -205.2, corresponding to 71 interface residues, involved into the complexation (Table 1). This indicates a strong interaction between HSA and Lz, suggesting a potential stabilizing effect of Lz on the albumin structure and its ligand-binding properties. The formation of HSA-Lz complexes resulted in a reconfiguration of the ligand binding domains, thereby modulating the binding affinity for specific TCC molecules.

Table 1. Interfacial amino acids and interaction modes for TCC binding in albumin-lysozyme complexes

TCC	HSA-Lz-TCC interface residues		Type of interactions
	HSA	Lz	
TcSES	THR_{420B*}, PRO_{421B}, GLU_{505B}, THR_{506B}, PHE_{507B}, THR_{508B}, PHE_{509B}, ASP_{512B}, LEU_{516B}, GLU_{520B}, ILE_{523B}, LYS_{524B}, THR_{527B}, ALA_{528B}, GLU_{531B}, PHE_{551B}	LYS_{33}, TRP_{34}, ARG_{115}, GLN_{123}, TYR_{124}	Hydrophobic interactions, hydrogen bonds

TCC	HSA-Lz-TCC interface residues		Type of interactions
	HSA	Lz	
TcTET	ASN_{109B}, ARG_{114B}, LEU_{115B}, GLU_{425B}, GLU_{520B}, ILE_{523B}, LYS_{524B}	TRP_{34}, ARG_{115}	Hydrophobic interactions, hydrogen bonds
TcMED	VAL_{116B}	GLU_{35}, ASN_{44}, ASN_{46}, SER_{51}, ASP_{53}, GLN_{58}, ILE_{59}, ASN_{60}, TRP_{64}, ALA_{108}, TRP_{109}, VAL_{110}, ALA_{111}	Hydrogen bonds
TcMAG	ASP_{107A}, ASP_{108A}, ASN_{109A}, ARG_{145A}, HSD_{146A}, PRO_{147A}, TYR_{148A}, LYS_{190A}, ALA_{191A}, SER_{193A}, ALA_{194A}, ARG_{197A}, GLU_{425A}, ASN_{458A}, GLN_{459A}		Hydrogen bonds, salt bridges
TcEXA	LEU_{115A}, VAL_{116A}, ARG_{117A}, PRO_{118A}, MET_{123A}, PHE_{134A}, LYS_{137A}, TYR_{138A}, LEU_{139A}, GLU_{141A}, ILE_{142A}, ARG_{145A}, TYR_{161A}, PHE_{165A}, LEU_{182A}, ARG_{186A}		Hydrophobic interactions, hydrogen bonds
TcECD	LEU_{115B}, ARG_{117B}, PRO_{118B}, MET_{123B}, PHE_{134B}, LYS_{137B}, TYR_{138B}, GLU_{141B}, ILE_{142B}, TYR_{161B}, LEU_{182B}, ASP_{183B}, LEU_{185B}, ARG_{186B}	ALA_{47}	Hydrophobic interactions, hydrogen bonds, salt bridges
TcDMSA	LEU_{115A}, VAL_{116A}, ARG_{117A}, PRO_{118A}, MET_{123A}, TYR_{138A}, ILE_{142A}, HSD_{146A}, PHE_{149A}, LEU_{154A}, PHE_{157A}, TYR_{161A}, LEU_{182A}, LEU_{185A}, ARG_{186A}, ASP_{187A}, GLY_{189A}, LYS_{190A}		Hydrogen bonds, salt bridges
TcDIS	GLU_{505B}, HSD_{510B}, LYS_{524B}, THR_{527B}	ARG_5, LYS_{33}, TRP_{34}, TYR_{38}, GLN_{123}, TYR_{124}	Hydrophobic interactions, hydrogen bonds, salt bridges
TcPER	TYR_{30B}, HSD_{67B}, THR_{68B}, PHE_{70B}, GLY_{71B}, LEU_{74B}, GLU_{95B}, ARG_{98B}, ASN_{99B}, PHE_{102B}		Hydrogen bonds
TcDTPA	LEU_{115A}, VAL_{116A}, ARG_{117A}, PRO_{118A}, MET_{123A}, PHE_{134A}, LEU_{135A}, LYS_{137A}, TYR_{138A}, GLU_{141A}, ILE_{142A}, TYR_{161A}, LEU_{182A}, ARG_{186A}		Hydrogen bonds, salt bridges
TcHYN	GLU_{383A}, LEU_{387A}, ASN_{391A}, LEU_{394A}, ALA_{406A}, LEU_{407A}, VAL_{409A}, ARG_{410A}, TYR_{411A}, LYS_{414A}, LEU_{430A}, LEU_{453A}, SER_{489A}, GLU_{492A}, LYS_{541A}, GLU_{542B}, LYS_{545A}		Hydrogen bonds, π-stacking, salt bridges
TcMEB	THR_{420B}, PRO_{421B}, ASN_{503B}, GLU_{505B}, THR_{506B}, HSD_{510B}, LYS_{524B}, THR_{527B}, GLU_{531B}	ARG_5, LYS_{33}, TRP_{34}, TYR_{38}, ARG_{115}, GLN_{123}, TYR_{124}	Hydrophobic interactions, hydrogen bonds, salt bridges

*-A and B denote monomer subunits of the HSA dimer

As illustrated in Fig. 1, right panel, the most pronounced changes in binding affinity were observed for TcMEB, with a less pronounced effect for TcDTPA. This suggests that the presence of Lz may induce conformational perturbations in HSA, exposing or altering binding sites that favor specific TCCs.

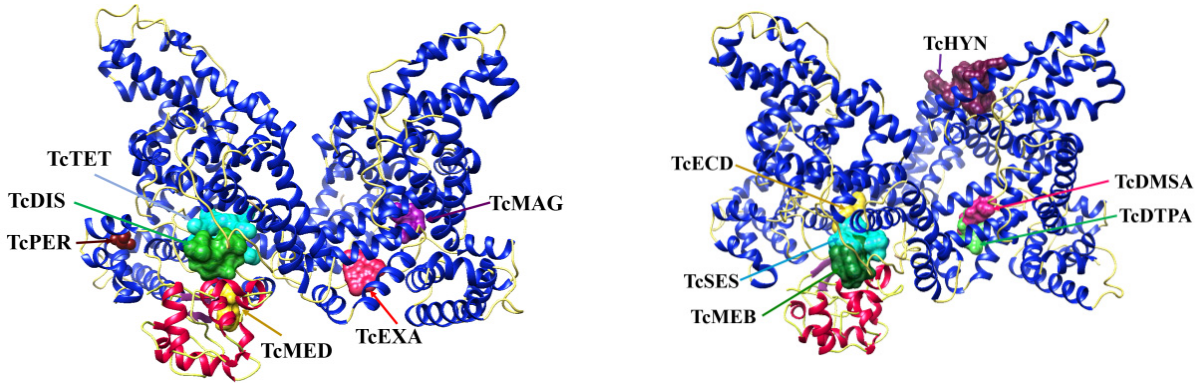

Figure 2. Structures of the most stable TCC complexes with HSA-Lz assemblies

The binding sites for TcMEB and TcDIS in the HSA-Lz complexes differ significantly from those on albumin alone, involving residues from both HSA and Lz. Specifically, interaction domain involves GLU_{505}, HSD_{510}, LYS_{524}, THR_{527} of HSA and ARG_5, LYS_{33}, TRP_{34}, TYR_{38}, GLN_{123}, TYR_{124} of Lz (Fig. 2). These findings imply that Lz may act as a structural modulator of HSA, potentially facilitating cooperative binding interactions between the two proteins and their ligands.

To further investigate the impact of Lz on drug delivery systems, we employed a multiple ligand docking approach to explore ternary ((HSA/HSA-Lz)-TCC-DOX) and quaternary (protein-TCC-DOX-FD) protein-ligand systems. The ternary systems were obtained by docking doxorubicin (DOX) to the best-score complexes of TCC with HSA and HSA-Lz (Fig. 3).

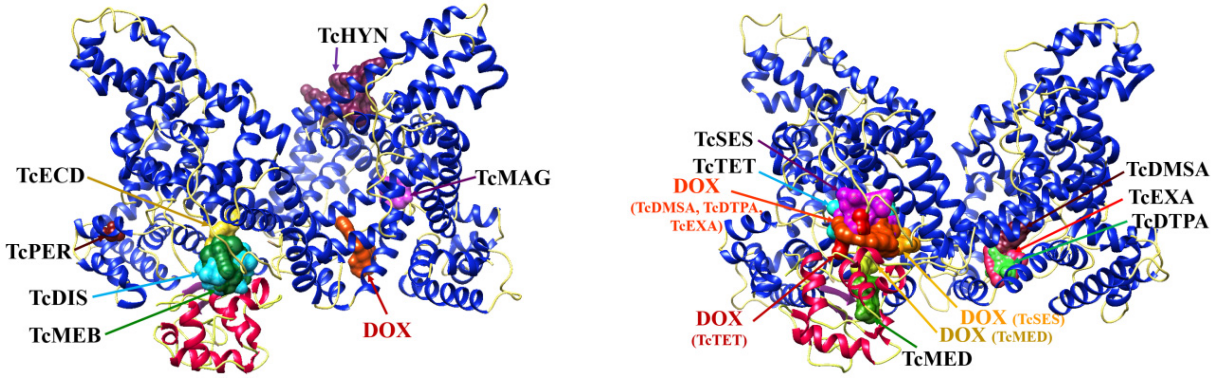

Figure 3. The highest affinity binding sites for DOX in the HSA-Lz-TCC systems

The following features of the ternary systems are worthy of mention: i) when the binding sites for TCC and DOX on HSA do not overlap, DOX binds to a site within domain I of the HSA molecule, spanning 16 residues between PRO_{113} and ARG_{186} (designated as site $HSA_{113\text{-}186}$); ii) when the binding sites overlap, as seen with TcMED, TcEXA, TcDMSA, and TcDTPA, DOX binds to an alternative site on HSA that includes 23 amino acid residues between ASP_{107} and GLN_{459}; iii) presence of Lz slightly enhances DOX binding affinity only in systems with TcTET and TcMED; iv) in systems containing Lz, DOX binds to site HSA113-186 in the absence of TCC and with TcMAG, TcECD, TcDIS, TcPER, TcHYN, and TcMEB. However, with other TCCs, the DOX binding site involves residues from both HSA and Lz. These results suggest that Lz may have a stabilizing effect on specific DOX binding sites, possibly due to alterations in protein conformational dynamics or indirect allosteric effects. The presence of Lz appears to promote a more defined and stable binding environment for DOX in certain ternary complexes, potentially influencing drug release kinetics and bioavailability. Further molecular dynamics simulations would be required to elucidate whether these observed changes are due to direct electrostatic interactions, hydrogen bonding stabilization, or shifts in protein secondary structure upon complex formation.

To achieve systems with dual imaging modalities, the best-score protein-TCC-DOX complexes were docked with NIR fluorophores, including methylene blue (MB), indocyanine green (IG), heptamethine cyanine dye AK7-5, and squaraine dye SQ1. Comparison of the docking results for quaternary systems (protein + TCC + DOX + FD) shows that the affinities of the examined dyes for HSA/HSA-DOX decrease in the following order: IG (BDS = -207.2 / -190.3) > SQ1 (BDS = -186.1 / -185.9) > AK7-5 (BDS = -162.4 / -162.9) > MB (BDS = -127.1 / -117.3). While the amino acid composition of FD binding sites varies among different TCCs and protein components, key residues that predominantly interact with FD can be identified. Notably, the albumin site spanning 12 residues between LEU_{115} and ARG_{186} (site $HSA_{115\text{-}186}$) is the preferred site for MB binding in HSA-DOX, HSA-TCC-DOX, and HSA-Lz-DOX complexes. In contrast, MB binding sites in HSA-Lz-TCC-DOX systems involve residues from both HSA and Lz (Table 2).

Table 2. The interface amino acid residues and the types of interactions involved in the binding of MB to HSA-Lz-TCC-DOX complexes

Complex	HSA-Lz-TCC- DOX-MB interface residues		Type of interactions
	HSA	LYS	
HSA-Lz-MB	LEU_{115A*}, VAL_{116A}, ARG_{117A}, PRO_{118A}, VAL_{122A}, MET_{123A}, ALA_{126A}, PHE_{134A}, LYS_{137A}, TYR_{138A}, GLU_{141A}, ILE_{142A}, TYR_{161A}, ARG_{186A}		Hydrophobic interactions, π-stacking
HSA-Lz-DOX-MB	VAL_{116B}, ARG_{117B}, PRO_{118B}	GLU_{35}, ASN_{44}, ASN_{46}, ASP_{53}, GLN_{58}, ASN_{60}, ARG_{62}, TYR_{63}, TRP_{64}, ALA_{108}, TRP_{109}, VAL_{110}	Hydrophobic interactions, π-stacking
HSA-Lz-TcSES-DOX-MB	ARG_{117B}, MET_{123B}, PHE_{134B}, LYS_{137B}, TYR_{138B}, GLU_{141B}, ILE_{142B}		Hydrophobic interactions
HSA-Lz-TcTET-DOX-MB	THR_{243B}, GLY_{248B}	LYS_{33}	Hydrophobic interactions
HSA-Lz-TcMED-DOX-MB	VAL_{116B}, ARG_{117B}, PRO_{118B}	GLU_{35}, ASN_{44}, ASN_{46}, ASP_{53}, GLN_{58}, ASN_{60}, ARG_{62}, TYR_{63}, TRP_{64}, ALA_{108}, TRP_{109}, VAL_{110}	Hydrophobic interactions, π-stacking
HSA-Lz-TcMAG-DOX-MB	VAL_{116B}, ARG_{117B}, PRO_{118B}	GLU_{35}, ASN_{44}, ASN_{46}, ASP_{53}, GLN_{58}, ASN_{60}, ARG_{62}, TYR_{63}, TRP_{64}, ALA_{108}, TRP_{109}, VAL_{110}	Hydrophobic interactions, π-stacking
HSA-Lz-TcEXA-DOX-MB	PRO_{421B}, HSD_{510B}, LYS_{524B}		Hydrophobic interactions

Complex	HSA-Lz-TCC- DOX-MB interface residues		Type of interactions
	HSA	LYS	
HSA-Lz-TcECD-DOX-MB	VAL_{116B}, ARG_{117B}, PRO_{118B}	GLU_{35}, ASN_{44}, ASN_{46}, ASP_{53}, GLN_{58}, ASN_{60}, ARG_{62}, TYR_{63}, TRP_{64}, ALA_{108}, TRP_{109}, VAL_{110}	Hydrophobic interactions, π-stacking
HSA-Lz-TcDMSA-DOX-MB	VAL_{116B}, ARG_{117B}, PRO_{118B}	GLU_{35}, ASN_{44}, ASN_{46}, ASP_{53}, GLN_{58}, ASN_{60}, ARG_{62}, TYR_{63}, TRP_{64}, ALA_{108}, TRP_{109}, VAL_{110}	Hydrophobic interactions, π-stacking
HSA-Lz-TcDIS-DOX-MB	VAL_{116B}, ARG_{117B}, PRO_{118B}	GLU_{35}, ASN_{44}, ASN_{46}, ASP_{53}, GLN_{58}, ASN_{60}, ARG_{62}, TYR_{63}, TRP_{64}, ALA_{108}, TRP_{109}, VAL_{110}	Hydrophobic interactions, π-stacking
HSA-Lz-TcPER-DOX-MB	VAL_{116B}, PRO_{118B}	GLU_{35}, ASN_{44}, ASN_{46}, ASP_{53}, GLN_{58}, ASN_{60}, ARG_{62}, TYR_{63}, TRP_{64}, ALA_{108}, TRP_{109}, VAL_{110}	Hydrophobic interactions, π-stacking
HSA-Lz-TcDTPA-DOX-MB	PRO_{421B}, HSD_{510B}, LYS_{524B}		Hydrophobic interactions
HSA-Lz-TcHYN-DOX-MB	VAL_{116B}, ARG_{117B}, PRO_{118B}	GLU_{35}, ASN_{44}, ASN_{46}, ASP_{53}, GLN_{58}, ASN_{60}, ARG_{62}, TYR_{63}, TRP_{64}, ALA_{108}, TRP_{109}, VAL_{110}	Hydrophobic interactions, π-stacking
HSA-Lz-TcMEB-DOX-MB	VAL_{116B}, ARG_{117B}, PRO_{118B}	GLU_{35}, ASN_{44}, ASN_{46}, ASP_{53}, GLN_{58}, ASN_{60}, ARG_{62}, TYR_{63}, TRP_{64}, ALA_{108}, TRP_{109}, VAL_{110}	Hydrophobic interactions, π-stacking

*-A and B denote monomer subunits of the HSA dimer

A remarkable characteristic of the HSA binding sites for IG is the consistent presence of three identical amino acid residues: ARG_{114A}, PRO_{421A} (with the exception of the system involving TcEXA), and ILE_{523A}. In contrast, the IG binding sites within HSA-Lz-TCC-DOX systems exhibit a higher degree of heterogeneity (Fig. 4). This observation suggests that Lz may introduce variability in fluorophore binding preferences, possibly due to subtle changes in local electrostatic potential or steric hindrance effects.

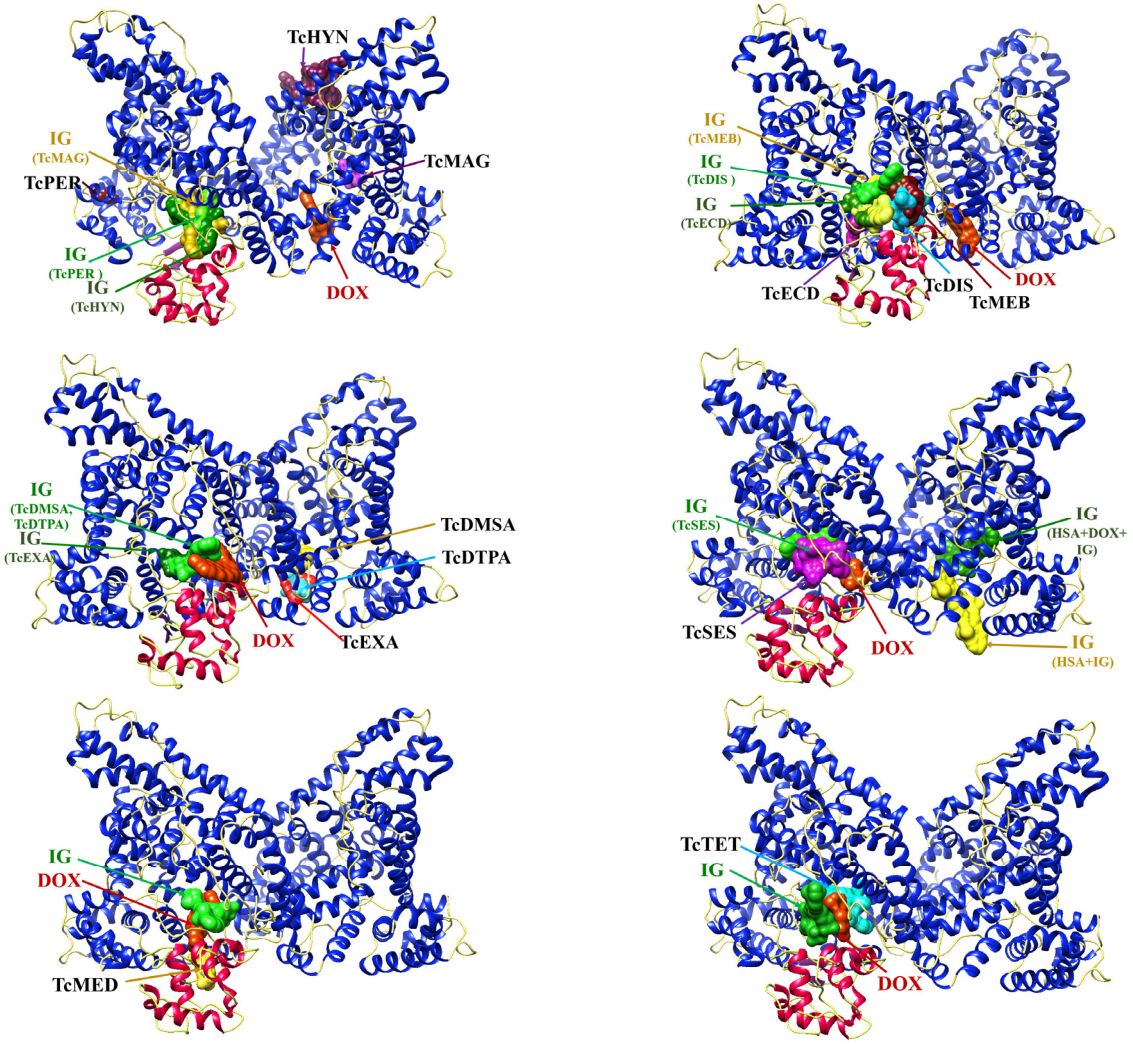

Figure 4. The most energetically favorable docking poses in the complexes HSA-Lz-TCC-DOX-IG

Notably, IG binding affinities are markedly higher in Lz-containing systems compared to HSA alone. This enhanced affinity could be attributed to the structural modifications induced by Lz, which may expose additional binding sites or alter the electrostatic properties of the protein surface. The interaction of AK7-5 with HSA occurs through sites composed of 18 (site HSA115-523) or 12 amino acid residues from albumin domains I and III, with the most pronounced increases in binding affinity observed in the systems HSA-Lz-TcSES-DOX and HSA-Lz-TcTET-DOX. These findings highlight the potential role of Lz in modulating fluorescence imaging properties within dual-modality drug delivery systems, opening avenues for further optimization and experimental validation.

Our findings support the hypothesis that the incorporation of lysozyme into albumin-based drug delivery systems can enhance the specificity and stability of TCC and NIR fluorophore binding. The observed changes in binding affinities and sites may be attributed to the structural and electrostatic modifications induced by Lz, which could influence the pharmacokinetics and targeting efficiency of these systems. Further experimental validation is necessary to confirm these hypotheses and explore the potential therapeutic benefits of these hybrid systems. The molecular mechanisms underlying these interactions may involve conformational changes in the protein structure upon complexation with Lz, which could expose new binding sites or alter the accessibility of existing ones. Additionally, the electrostatic properties of the protein surface may be modified, influencing the binding affinities of TCC and NIR fluorophores. These modifications could enhance the stability and specificity of the delivery system, potentially improving its therapeutic efficacy and reducing systemic toxicity.

CONCLUSIONS

Taken together, the results of this study suggest that Lz-containing drug delivery systems may offer enhanced stability and altered binding characteristics for both radionuclide and fluorescent imaging agents. The cooperative interactions observed between HSA and Lz could be further explored to develop novel multimodal nanocarriers with improved pharmacokinetics and targeting capabilities. Future work should focus on molecular dynamics simulations and experimental binding assays to validate the observed docking trends and assess the potential of these systems for clinical translation.

Acknowledgements

This work was supported by the Ministry of Education and Science of Ukraine (the project № ДЗ/174-2025).

ORCID IDs

Valeriya Trusova, https://orcid.org/0000-0002-7087-071X; **Uliana Malovytsia,** https://orcid.org/0000-0002-7677-0779
Galyna Gorbenko, https://orcid.org/0000-0002-0954-5053; **Andrey Zelinsky,** https://orcid.org/0000-0002-4110-8523
Borys Borts, https://orcid.org/0000-0002-1492-4066; **Pylyp Kuznietsov,** https://orcid.org/0000-0001-8477-1395
Ivan Yakymenko, https://orcid.org/0000-0001-8477-1395

REFERENCES

[1] C. Li, Z. Wang, H. Lei, and D. Zhang, Drug Deliv. **30**, 2174206 (2023). https://doi.org/10.1080/10717544.2023.2174206
[2] P. Trucillo, Processes **9**, 470 (2021). https://doi.org/10.3390/pr9030470
[3] A. Spada, J. Emami, J. Tuszynski, and A. Lavasanifar, The uniqueness of albumin as a carrier in nanodrug delivery, Mol. Pharmaceut. 18, 1862. https://doi.org/10.1021/acs.molpharmaceut.1c00046
[4] V. Trusova, U. Tarabara, I. Karnaukhov, A. Zelinsky, B. Borts, I. Ushakov, L. Sidenko, and G. Gorbenko, East Eur. J. Phys. (4), 447 (2024). https://doi.org/10.26565/2312-4334-2024-4-54
[5] V. Trusova, U. Malovytsia, P. Kuznietsov, I. Karnaukhov, A. Zelinsky, B. Borts, I. Ushakov, *et al*., East Eur. J. Phys. (1), 376 (2025). https://doi.org/10.26565/2312-4334-2025-1-46
[6] R. Halaby, Cancer Drug Resist. **2**, 31 (2019). http://dx.doi.org/10.20517/cdr.2018.23
[7] B. Zhitomirsky, and Y. Assaraf, Oncotarget, **8**, 45117 (2017). http://dx.doi.org/10.18632/oncotarget.15155
[8] I. Schadt, and V. Marino, Curr. Res. Cmpl. Alt. Med. **7**, 188 (2023). https://doi.org/10.29011/2577-2201.100088
[9] P. Ojha, N. Kar, H. Behera, M. Parija, S. Nayak, S. Singh, A. Patra, and K. Sahoo, Biotech. **13**, 240 (2023). https://doi.org/10.29011/2577-2201.100088
[10] M.F. Adasme, K.L. Linnemann, S.N. Bolz, F. Kaiser, S. Salentin, V.J. Haupt, and M. Schroeder, Nucl. Acids Res. **49**, W530-W534 (2021). https://doi.org/10.1093/nar/gkab294

КОМП'ЮТЕРНЕ ДОСЛІДЖЕННЯ СИСТЕМ ДОСТАВКИ ЛІКІВ З РАДІОНУКЛІДНИМИ ТА ФЛУОРЕСЦЕНТНИМИ МОДАЛЬНОСТЯМИ ВІЗУАЛІЗАЦІЇ. ІІІ. СИСТЕМИ НА ОСНОВІ АЛЬБУМІНУ ТА ЛІЗОЦИМУ ДЛЯ ДОСТАВКИ ДОКСОРУБІЦИНУ

В. Трусова[a], У. Маловиця[a], П. Кузнєцов[b], І. Якименко[b], І. Карнаухов[c], А. Зелінський[c], Б. Борц[c], І. Ушаков[c], Л. Сіденко[c], Г. Горбенко[a]

[a]Кафедра медичної фізики та біомедичних нанотехнологій, Харківський національний університет імені В.Н. Каразіна м. Свободи 4, Харків, 61022, Україна
[b]Кафедра фізики ядра та високих енергій імені О.І. Ахієзера, Харківський національний університет імені В.Н. Каразіна м. Свободи 4, Харків, 61022, Україна
[c]Національний науковий центр «Харківський фізико - технічний інститут», Харків, вул. Академічна, 1, 61108, Україна

Дане дослідження присвячене розробці білкових систем доставки лікарських засобів для доксорубіцину (DOX) шляхом інтеграції лізоциму в носії на основі альбуміну, що включають як радіонуклідні (комплекси технецію-99m), так і флуоресцентні (барвники ближнього інфрачервоного діапазону) методи візуалізації. Використовуючи метод молекулярного докінгу, було досліджено спорідненість зв'язування та сайти комплексів технецію-99m і флуоресцентних барвників ближнього інфрачервоного діапазону в гібридних білкових системах. Результати демонструють, що включення лізоциму суттєво модулює ландшафт зв'язування, підвищуючи специфічність і стабільність комплексів технецію та флуоресцентних барвників. Зокрема, спорідненість зв'язування індоціаніну зеленого була значно вищою в системах, що містять лізоцим, що свідчить про покращення можливостей візуалізації. Крім того, аналіз виявив різні сайти зв'язування для доксорубіцину в присутності різних комплексів технецію, що може впливати на вивільнення препарату та його терапевтичну ефективність. Ці результати підтверджують потенціал гібридних систем альбумін-лізоцим як наноносіїв із подвійними можливостями візуалізації для доставки DOX, пропонуючи перспективний підхід до підвищення терапевтичної ефективності при одночасному зниженні системної токсичності в протиракову лікуванні та сприяючи розробці більш складних і цільових платформ доставки для терапії раку.

Ключові слова: *наносистеми доставки ліків на основі білків; людський сироватковий альбумін; лізоцим; доксорубіцин; комплекси технецію; інфрачервоні барвники; молекулярний докінг*